J. Fluid Mech. (1981), *vol.* 112, *pp.* 97–125
Printed in Great Britain

An unsteady lifting line theory of flapping wings with application to the forward flight of birds

By P. J. PHLIPS†, R. A. EAST AND N. H. PRATT

Department of Aeronautics and Astronautics, University of Southampton, Southampton S09 5NH, U.K.

(Received 10 December 1980)

A lifting line theory of flapping wings in steady forward flight is presented in which the unsteady features of the flow are modelled. A detailed three-dimensional model of the vortex wake is used to evaluate the unsteadiness to first order. The method gives satisfactory agreement with well-known limiting cases. Relationships between the geometric and the kinematic parameters, and the forces and the power are predicted which are compatible with the limited experimental evidence. The theory is applied to the calculation of the power curve of specific birds. Important similarities and differences are observed between the present results and those of Pennycuick (1975) and Rayner (1979*c*).

1. Introduction

Continuous circular motion is rarely found in nature and as a consequence avian and aquatic propulsion are usually effected by the reciprocation of aerodynamic/hydrodynamic surfaces about which a circulation is established. This results in a component of force in the desired direction of motion. For avian flight aerodynamic lift is also required to sustain motion in the atmosphere; this may also be achieved by flapping surfaces or, at sufficiently high speed, by gliding motion. In most man-made air-breathing flying vehicles, on the other hand, propulsion is achieved by some form of steady or quasi-steady flow propulsor employing propellers, rotors, turbines, etc., spinning about an axis, as in the case of fixed wing aircraft and helicopters. Notable exceptions are the ornithopter and the pulse-jet, each of which employ non-steady flow processes.

A complete and exact analysis of flapping flight is probably one of the most complex goals to be attempted in flight mechanics. Indeed, birds, the most successful practitioners of this mode of transport, use a complex interaction between viscous and inviscid non-steady aerodynamics, variable geometry flexible surfaces of variable porosity, together with rapid-response adaptive biological systems, to achieve their outstanding results. This complexity has so far prevented any exact modelling of avian flight mechanics, although progress has been made by adapting the classical mechanics of flight model (see, for example, Etkin 1972) for conventional fixed wing aircraft to this problem. The most widely used model of this type is that of Pennycuick (1968), which has been modified by Tucker (1973). Subsequent variations on the basic

† Present address: Department of Aeronautics and Astronautics, MIT, Cambridge, Massachusetts.

model have been summarized by Pennycuick (1975). A review of bird flight analyses has been presented by Lighthill (1977) and more recently by Rayner (1979*b*).

In Pennycuick's model the forces which sustain and propel result from an assumed actuator disk and the associated steady momentum flux, similar in concept to the simple model of a vectored thrust aircraft or helicopter. The model ignores, however, the essential feature of flapping as a reciprocating and hence intermittent integrated lifting and propulsive mechanism for which the generated forces result from an unsteady momentum flux. Nevertheless, useful parametric results may be obtained from such theoretical models, particularly with regard to the power characteristics.

The essential implicit assumption of models based on an actuator disk is the steady nature of the momentum flux, often referred to as the vortex wake, associated with the forces produced. These models therefore ignore the periodic variation of the vortex wake and the associated periodic aerodynamic loading on flapping wings. Wagner (1925) showed that the lift on an infinite-aspect-ratio wing impulsively started from rest took several chord lengths to reach a steady value because of the induced velocity field from the starting vortex. Similarly, each major change of aerodynamic loading which occurs at the extremities of the periodic motion of a flapping wing results in the formation of transverse vortices in the wake analogous to the starting vortex. These vortices have been observed by Wood & Kirmani (1970) in the wake of a heaving aerofoil and by Kokshaysky (1979) in the wake of a flying bird. For wings of chord c^* flapping with angular frequency ω and moving at speed U, the vortex associated with the change of aerodynamic loading plays an increasing role in determining the rate of increase of the aerodynamic forces as the wing moves away from the vortex for increasing values of the frequency parameter $\omega c^*/U$. Vortices shed on earlier cycles of the motion also influence the downwash field in the vicinity of the flapping surface but with a progressively diminishing magnitude. It is therefore to be expected that, as a consequence of these essentially non-steady phenomena, the average forces on a flapping wing would be significantly different from those predicted by any method based on steady momentum flux principles. Indeed, recent measurements by Cloupeau, Devillers & Devezeaux (1979) of the instantaneous lift in the desert locust *Schistocerca gregaria* flying in a wind tunnel have experimentally confirmed the existence of significant unsteady effects.

Betteridge & Archer (1974) for rigid wings and Archer, Sapuppo & Betteridge (1979) for flexible wings have included the periodic nature of the aerodynamic forces by applying the classical lifting line method to flapping wings. They calculated the induced velocity at the lifting line from a quasi-steady model of the wake. This method therefore excluded the unsteady features of the vortex wake which the results of the present work show to be important.

More recently, Rayner (1979*a*, *b*, *c*) has modelled both hovering and forward flapping bird flight by using a more relevant model of the vortex wake. This model is based on the assumption that the wing is aerodynamically loaded only during the downstroke and that the associated shed vorticity rolls into a series of closed elliptic vortex loops. This model would seem to have good application to hovering and flight at low forward speeds. At higher speeds a small correction may be required since Brown (1953) has shown that at medium and high speeds the wing may also be aerodynamically loaded during the upstroke but to a lesser extent than during the downstroke.

Many aspects of flapping flight therefore remain to be correctly modelled. In particular, no attempt has yet been made to include an adequate description of the effect of the unsteady vortex wake on the aerodynamic loading of flapping wings, although Cone (1968) formulated such a model which proved too complicated for solution. One of the aims of the present work is to consider this effect by presenting an approximate description of the unsteady wake. It is detailed enough to represent the three-dimensional wake, yet simple enough for the induced velocity field to be evaluated numerically. By using this model wake, together with lifting line theory, a detailed unsteady spanwise loading distribution on the flapping wing is deduced and the input power required is obtained by considering the torque about the wing hinge. The motivation for this work has been to examine the importance of unsteady flow effects in flapping flight.

As a detailed description of bird flight, the model is probably over-simplified because a number of effects, such as viscosity, porosity, variable geometry, etc., have not been included. Also, no attempt has been made to account for the efficiency of energy conversion between input and output of the bird's flight muscles. However, in order to illustrate the possible effect of unsteady aerodynamic phenomena on avian flight mechanics, sample calculations of the power consumption and cost of transport for typical bird geometries are presented.

2. Definitions and assumptions

The flapping model is essentially that adopted by Lighthill (1977). Consider a pair of flapping wings flying at constant altitude and with a steady speed U. They are hinged about a longitudinal axis (body axis) which makes an angle θ with the flight path, as shown diagrammatically in figure 1. The wings are assumed to flap in a plane perpendicular to this axis. Two right-handed co-ordinate systems are defined: one is the conventional ($\mathbf{i}$, $\mathbf{j}$, $\mathbf{k}$) system, the other, ($\mathbf{l}$, $\mathbf{m}$, $\mathbf{n}$), is defined relative to the moving wings. The wings are at an incidence α_0 relative to the body axis. The total angular amplitude of flapping is β, about a mean angle γ. The instantaneous angle between the wing and the horizontal is $\phi(t)$; the angular velocity of flapping, $\dot{\phi}$, is taken to be constant. The frequency of flapping is f and the angular frequency $\omega = 2\pi f$. The wing semispan is s, the radial distance is r^*, $0 < r^* < s$, and the wing chord is $c^*(r^*)$.

Let us now define the scope of our investigation more precisely by making the following assumptions. We restrict ourselves to rigid, non-porous, unswept wings of high aspect ratio. We assume that the fluid is incompressible and that the Reynolds number is high. The flow can then be considered to consist of an inner viscous region, the boundary layer, and an outer inviscid region. In this paper we consider the inviscid flow and use aerofoil theory to determine the resultant aerodynamic forces on the wings. It is clear that, since we ignore the viscous region and the possible coupling effects between the two regions, our inviscid theory is only a partial solution to the problem at hand. The study of the viscous effects leading to the determination of the profile drag in an unsteady flow, and the dynamic stall are topics for further investigation.

Following Robinson & Laurmann (1956), in an unsteady flow we may express the resultant aerodynamic force per unit span $\mathbf{N}(t)$ normal to the relative velocity $\mathbf{V}^*(t)$ by the series

$$\mathbf{N} = f(\alpha, \mathbf{V}^*) + g(\dot{\alpha}, \dot{\mathbf{V}}^*) + h(\ddot{\alpha}, \ddot{\mathbf{V}}^*) + \dots,$$

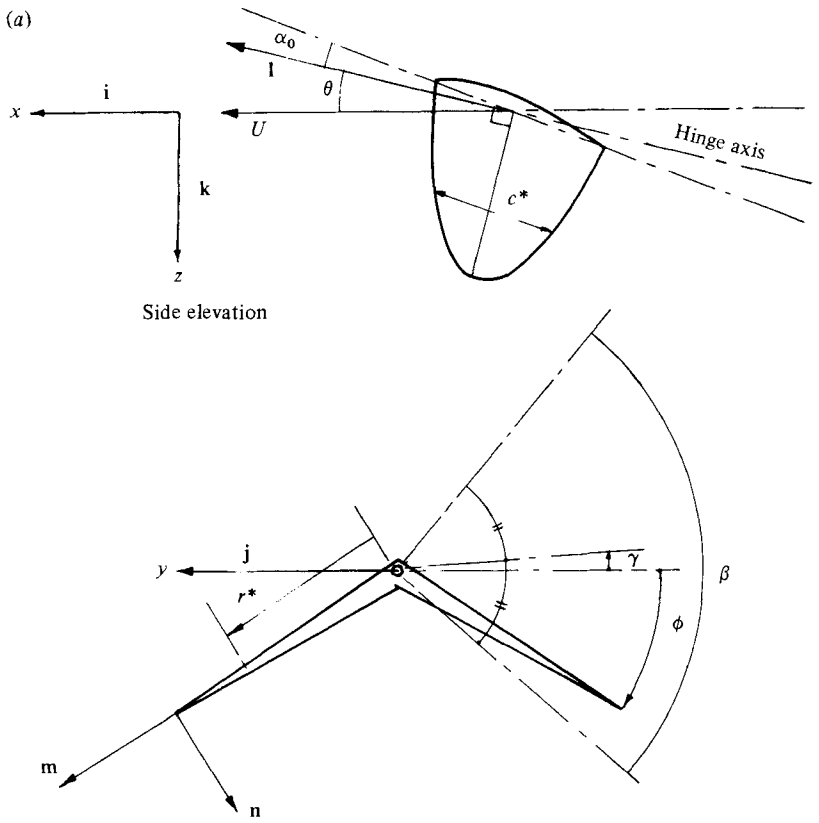

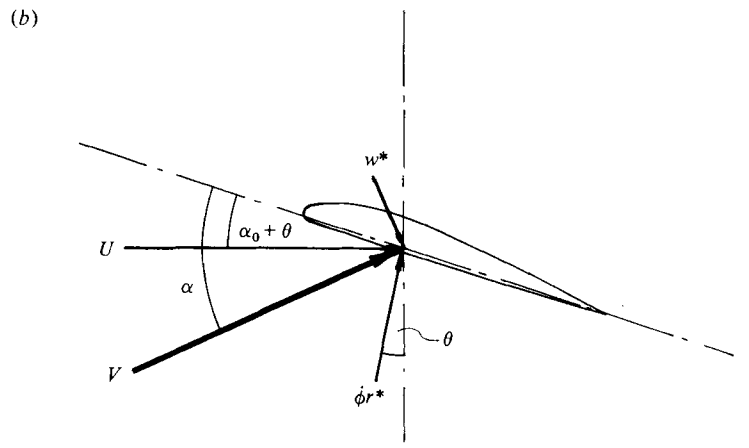

FIGURE 1(*a*). Diagram of the flapping wing showing co-ordinate systems. (*b*) Diagram of the velocities relative to the wing in a plane normal to the wing span axis **m**. V is the resultant of the forward velocity U, the flapping velocity $\dot{\phi} r^*$ and the induced velocity w^*.

where $\alpha(t)$ is the incidence. In the present study we shall assume that the flapping frequency is low and consider only the first term, $\mathbf{N} \simeq f(\alpha, \mathbf{V}^*)$. The first-order unsteady effects are those resulting from the variations of the velocity and the incidence due to the flapping motion and the unsteady induced velocities. The neglected $\dot{\alpha}$ and $\dot{\mathbf{V}}^*$ terms, the dynamic viscous effects and the virtual mass effects, are assumed to be small.

To avoid ambiguities, some other terms used throughout this study are defined below. The lift L and the thrust T are defined as the components of the resultant aerodynamic force perpendicular to and in the direction of the flight velocity $\mathbf{U}$:

$$L(t) = -2\int_0^s \mathbf{k}.\mathbf{N}(r^*,t)\,dr, \qquad T(t) = 2\int_0^s \mathbf{i}.\mathbf{N}(r^*,t)\,dr. \tag{1}$$

In the case of aircraft the thrust is negative and is called the induced drag. It will be obvious that for a system propelling itself by flapping the notion of induced drag does not apply. Finally, the power P is defined as the rate at which the aerodynamic forces do work about the wing hinges (Betteridge & Archer 1974):

$$P(t) = \pm 2\dot{\phi}\int_0^s \mathbf{n}.\mathbf{N}(r^*,t)\,r^*\,dr^*. \tag{2}$$

3. The vortex wake

The above expressions for the lift, the thrust, and the power share one important factor, the local instantaneous normal force $\mathbf{N}(r^*,t)$. Classical aerofoil theory gives this as

$$\mathbf{N} = \rho\mathbf{V}^* \wedge \boldsymbol{\Gamma}^*, \tag{3}$$

where ρ is the fluid density, $\boldsymbol{\Gamma}^*$ is the circulation and both the induced velocity component $\mathbf{w}^*$ of $\mathbf{V}^*$ and the circulation $\boldsymbol{\Gamma}^*$ are unknown. They interact strongly, $\mathbf{w}^*$ being the result of changes in $\boldsymbol{\Gamma}^*$. It is, therefore, important to use a physically realistic model of the vortex wake in order to obtain satisfactory distributions of $\boldsymbol{\Gamma}^*$, L, T, P, etc. Since the flow is unsteady and we propose to obtain the average values of the forces and the power from time integration over a cycle, the model of the wake must be detailed enough to include the main unsteady features in addition to the three-dimensional spatial features.

Cone (1968) and Betteridge & Archer (1974) qualitatively describe the vortex wake as the surface traced out by the wings in their forward flapping motion, consisting of a grid of vortices. These are the vortices due to the spanwise circulation gradient, which we call streamwise vortices, and the vortices due to the variation of the circulation with time, called the transverse vortices. The above-mentioned authors found their model too complex to be of use in a quantitative analysis. Their model is of the wake as it would appear if the vorticity remained fixed in space after being shed from the wings. However, it is well known that vortices do move because of their mutual interactions. Hence, we may develop a model which retains the transverse and the streamwise vortices, but rearranges them into a spatial assembly suggested by the interaction of the vortices. This new simplified spatial arrangement is more amenable to quantitative treatment.

The wake of a high-aspect-ratio wing in steady flight consists of streamwise vortices only, and it is well known that they rapidly roll up into two discrete vortices. Wood

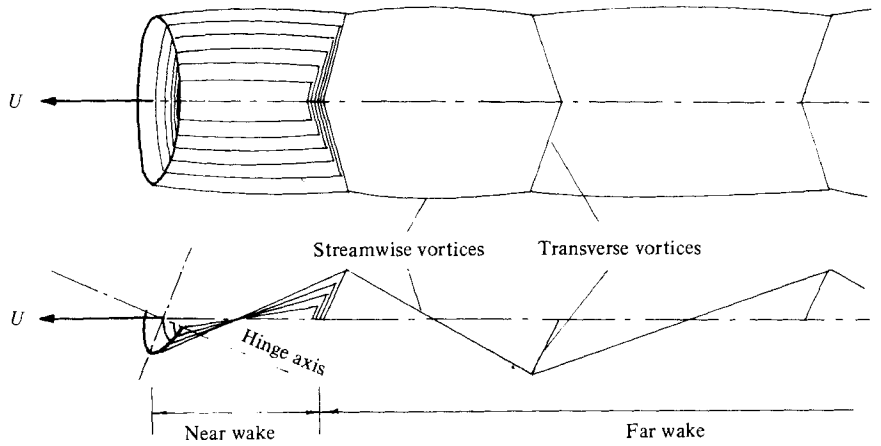

FIGURE 2. The vortex wake (schematic).

& Kirmani (1970) have shown that the wake of a heaving aerofoil consists of a series of discrete vortices arranged as a vortex sheet. For flapping wings, McRobert (1980), using a water tunnel, has demonstrated the existence of discrete periodic wake vortices and Kokshaysky (1979) has observed a somewhat similar vortex loop structure in the wake of a flying bird. This leads us to adopt a model of the wake consisting of two parts, as shown in figure 2: a near wake in which the vorticity has partly rolled up, and a far wake consisting of discrete vortices.

The near wake is the surface traced out by the wings during the stroke under consideration. A stroke is taken to start at the highest or lowest elevation of the wings. In the near wake, it is assumed that the streamwise vortices still form a vortex sheet. The transverse vorticity is collected at the position of the wings at the start of each stroke. The model thus ignores the subsequent distortion and convection of the wake; a standard assumption in steady wing theory. The hypothesis is that the velocity induced at the wings can be evaluated satisfactorily by assuming that the vortices stay in the stream surface in which they originated. This assumption clearly becomes invalid in the limit of low speeds. At low speeds a model taking into account the convection of the vortices, such as that of Rayner (1979*a*, *b*), is needed. In the numerical evaluation of the induced velocities, the curved line vortices were replaced by a succession of short straight line segments. Finally, we may point out that the modelling done here is similar in nature to that used in the case of helicopters; see Bramwell (1976).

4. Theory

The method developed below is based on the classical lifting line method, see for instance Duncan, Thom & Young (1970), but in the present work the symbols $\mathbf{V}^*$, Γ^*, L, etc., all represent instantaneous values. Although we follow the same steps as the classical theory, the form of the expression becomes quite different. This is due to the fact that in flapping flight we have no simple analytic relationship between the geometry of the wake and the induced velocity.

As shown in figure 1 (*b*) the relative velocity $\mathbf{V}^*$ has three components: the forward

velocity $-U\mathbf{i}$, the flapping velocity $\pm\dot{\phi}r^*\mathbf{n}$, and the induced velocity $\mathbf{w}^*$. Following Lighthill (1977), we write the $\mathbf{n}$ and $\mathbf{l}$ components of $\mathbf{V}^*$ as

$$\mathbf{V}^*.\mathbf{n} = -U\cos\phi\sin\theta \pm r^*\dot{\phi} + w_n^*, \quad \mathbf{V}^*.\mathbf{l} = -U\cos\theta + w_l^*.$$

In potential flow, the spanwise velocity $\mathbf{V}^*.\mathbf{m}$ has no effect on the forces and is therefore not considered. We now introduce the non-dimensional quantities c, r, $\mathbf{V}$, $\mathbf{w}$, and $\boldsymbol{\Gamma}$, defined as

$$c = c^*/s, \quad r = r^*/s, \quad \mathbf{V} = \mathbf{V}^*/U, \quad \mathbf{w} = \mathbf{w}^*/U, \quad \text{and} \quad \boldsymbol{\Gamma} = \boldsymbol{\Gamma}^*/Us.$$

The $\mathbf{n}$ and $\mathbf{l}$ components of $\mathbf{V}^*$ then become

$$\mathbf{V}.\mathbf{n} = V_n + w_{nn}, \quad \mathbf{V}.\mathbf{l} = V_l + w_{nl},$$

where

$$V_n = -\cos\phi\sin\theta \pm r\nu\frac{\beta}{\pi} + w_{fn}, \quad V_l = -\cos\theta + w_{fl},$$

and ν is the reduced frequency (or frequency parameter) defined by

$$\nu \equiv \omega s/U,$$

w_{fl} and w_{fn} are the $\mathbf{l}$ and $\mathbf{n}$ components of the far wake induced velocity, and w_{nl} and w_{nn} are the corresponding components of the near wake induced velocity. The velocity $\mathbf{w}_f$ is determined separately using approximate values for the vortex strength, found by using the present method with $\mathbf{w}_f = 0$ initially. The total velocity is, therefore, the sum of two known components, V_n and V_l, and two unknown components, w_{nl} and w_{nn}, the spanwise component being neglected.

We have two equivalent expressions for the magnitude N of the local normal force $\mathbf{N}$, viz.

$$N = \rho V^*\Gamma^* \quad \text{and} \quad N = \tfrac{1}{2}\rho(V^*)^2 S C_N,$$

the second being simply the dimensional relationship, where S is the wing area and $V^* = |\mathbf{V}^*|$. If we equate these two equations and take $C_N = 2\pi\alpha$, the theoretical value for thin aerofoils, where α is the effective incidence, we find that

$$\Gamma = \pi c\, V\alpha. \tag{4}$$

Now V and α are given by

$$V^2 = (V_n + w_{nn})^2 + (V_l + w_{nl})^2, \quad \alpha = \alpha_0 + \tan^{-1}\left(\frac{V_n + w_{nn}}{V_l + w_{nl}}\right).$$

We can make the approximations

$$V \simeq (V_n^2 + V_l^2)^{\frac{1}{2}}, \quad \alpha \simeq \alpha_0 + \frac{V_n + w_{nn}}{V_l}$$

on the assumptions that $w \ll V$, and that $\mathbf{V}.\mathbf{n} \ll \mathbf{V}.\mathbf{l}$. Substituting for V and α in equation (4) gives

$$\Gamma = E + Fw_{nn}, \tag{5}$$

where

$$E = \left(\alpha_0 + \frac{V_n}{V_l}\right)(V_n^2 + V_l^2)^{\frac{1}{2}} \quad \text{and} \quad F = \frac{\pi c}{V_l}(V_n^2 + V_l^2)^{\frac{1}{2}}$$

are known, whereas Γ and w_{nn} are as yet unknown. We represent the spanwise circulation distribution by a Fourier series, so that at a point P along the span

$$\Gamma(P) = \sum_{n=1}^{\infty} A_n \sin n\psi(P) = \sum_{n=1}^{\infty} A_n b_n, \tag{6}$$

where $\psi(P) = \cos^{-1} r(P)$ and $n = 1, 3, 5, \ldots$. This series satisfies the conditions that the loading must vanish at the wing tips, and must be symmetric about the centreline.

We must now relate the induced velocity w_{nn} to the circulation. We may begin with

$$w_{nn}(P) = \int_0^{\frac{1}{2}\pi} \frac{\partial w_{nn}(P, \psi)}{\partial \Gamma} \frac{\partial \Gamma(\psi)}{\partial \psi} d\psi, \tag{7}$$

in which the factor $\partial w_{nn}/\partial\Gamma$ is the velocity induced at a point P, per unit Γ, by the vortex loop leaving the trailing edge at $r = \cos\psi$. After substituting for $\partial\Gamma/\partial\psi$ obtained from (6), the induced velocity (7) becomes

$$w_{nn} = \sum_{n=1}^{\infty} nA_n d_n, \tag{8}$$

where

$$d_n = \int_0^{\frac{1}{2}\pi} \frac{\partial w_{nn}}{\partial \Gamma} \cos n\psi \, d\psi, \quad \text{and} \quad n = 1, 3, 5, \ldots .$$

The induced velocity per unit circulation $\partial w_{nn}/\partial\Gamma$ is evaluated numerically at $2N$ points along one wing, located at constant intervals $\Delta\psi = \pi/4N$. To evaluate the coefficients d_n we use Filon's (1928) formula for trigonometric quadratures and find that

$$d_n = (\zeta S_{2n} + \eta S_{2n-1})\,\Delta\psi, \tag{9}$$

where

$$\zeta = \frac{2(1+\cos^2 nh)}{(nh)^2} - \frac{4\sin nh \cos nh}{(nh)^3}, \quad \eta = \frac{4\sin nh}{(nh)^3} - \frac{4\cos nh}{(nh)^2}.$$

S_{2n} is the sum of the even ordinates of the curve $y = (\partial w_{nn}/\partial\Gamma)\cos n\psi$ between zero and $\frac{1}{2}\pi$ inclusive, less half the first and last ordinates, and S_{2n-1} is the sum of all the odd ordinates.

The final step is to combine equations (5), (6) and (8) to obtain a linear equation in the A_n's:

$$\sum_{n=1}^{N} (b_n - nd_n F) A_n = E. \tag{10}$$

It remains to solve (10) simultaneously at N points along one wing to obtain the first N coefficients of the Fourier series. The induced velocities can then be evaluated by using equation (8), so that both $\mathbf{V}$ and $\boldsymbol{\Gamma}$ can be calculated.

Using equations (1), (3) and (6), we find that the lift is

$$C_L = \frac{L}{\frac{1}{2}\rho U^2 S} = -A \sum_{n=1}^{\infty} A_n \int_0^{\frac{1}{2}\pi} ((\mathbf{V} \wedge \mathbf{m}).\mathbf{k}) \sin n\psi \sin\psi \, d\psi, \tag{11}$$

where $n = 1, 3, 5, \ldots$ and A is the aspect ratio, $A = 4s^2/S$. The expression for the thrust coefficient is similar, except that we take the dot product with $\mathbf{i}$ instead of $\mathbf{k}$. The classical lifting line results can be recovered from this equation since for rigid, non-flapping wings $\mathbf{m} = \mathbf{j}$, so that $(\mathbf{V} \wedge \mathbf{m}).\mathbf{k} = -1$. The lift coefficient is then

$$C_L = \tfrac{1}{4}\pi A A_1 \quad \text{and} \quad L = \tfrac{1}{2}\pi U s (U s A_1). \tag{12}$$

Noting that $\Gamma^* = Us\Sigma_{n=1}^{\infty} A_n \sin n\psi$, equation (12) is the classical lifting line result, derived for instance in Duncan *et al.* (1970). Similarly, if $\mathbf{w}$ is constant along the span then $-C_T = \frac{1}{4}\pi w A A_1$ is the aircraft's induced drag coefficient, so that $C_{D_i} = (w^*/U)C_L$, as in the classical theory.

In flapping flight, the x and z components of $(\mathbf{V} \wedge \mathbf{m})$ vary along the span and, therefore, all the terms of the Fourier series (6) are required in the evaluation of (11). This equation is of the same form as the equation for the coefficients d_n and, therefore, we again make use of Filon's formula, and find that

$$C_L = -Ah \sum_{n=1}^{2N-1} A_n(\zeta T_{2n} + \eta T_{2n-1}),$$

where $h = \pi/2N$, $n = 1, 3, 5, \ldots$, and ζ and η are defined as in equation (9), and T_{2n} and T_{2n-1} are defined in the same fashion as S_{2n} and S_{2n-1}. Similarly one can show that the expression for the power coefficient is

$$C_P = \frac{P}{\frac{1}{2}\rho U^3 S} = \frac{A\nu\beta}{2\pi} \sum_{n=1}^{\infty} A_n \int_0^{\frac{1}{2}\pi} \mathbf{V}.\mathbf{l} \sin n\psi \sin 2\psi \, d\psi,$$

which, using Filon's formula, becomes

$$C_P = \frac{Ah\nu\beta}{2\pi} \sum_{n=1}^{2N-1} A_n(\zeta U_{2n} + \eta U_{2n-1}),$$

where U_{2n} and U_{2n-1} are defined in terms of the function $\mathbf{V}.\mathbf{l} \sin n\psi \sin 2\psi$.

5. Numerical results

5.1. *Limiting cases*

The above theory has been coded in FORTRAN IV and numerical results have been obtained using Southampton University's ICL 2970 computer. Three limiting cases were examined to check, as far as possible, the validity and the accuracy of the program, the numerical method, and the model. The simplest limiting case is the rectangular, finite aspect ratio, untwisted wing in steady, non-flapping flight. This is simulated by using very small values of ν and β. The values of lift and induced drag obtained (not reproduced here) were within 0·5 % of the classical results (Duncan *et al.* 1970).

The impulsively started, non-flapping, finite-aspect-ratio wing provides a non-steady test case, in which we compare our results with those of Jones (1940). Only the circulatory lift is accounted for in the present method, that is the first term of the expansion $\mathbf{N} = f(\alpha, \mathbf{V}) + g(\dot{\alpha}, \dot{\mathbf{V}}) + \ldots$ and this correctly tends to zero at the start of the motion, as shown in figure 3. When $x/c^* \to \infty$, where x is the distance travelled, the lift tends to the value given by the lifting line theory. The lift calculated by Jones includes the second term $g(\dot{\alpha}, \dot{\mathbf{V}})$, which is the lift due to the pressure fields caused by the accelerations and rotations. At $x = 0$, this lift is equal to one half of the lift of a wing of infinite aspect ratio in steady flow. Hence, Jones' curve has a different value of the starting lift. In the limit of $x/c^* \to \infty$, the lift calculated by Jones remains 1·3 % below the lifting line value, but Jones provides no explanation for this discrepancy. The difference between the present results and those of Jones is attributed to the differences between the models rather than to numerical errors in our calculations.

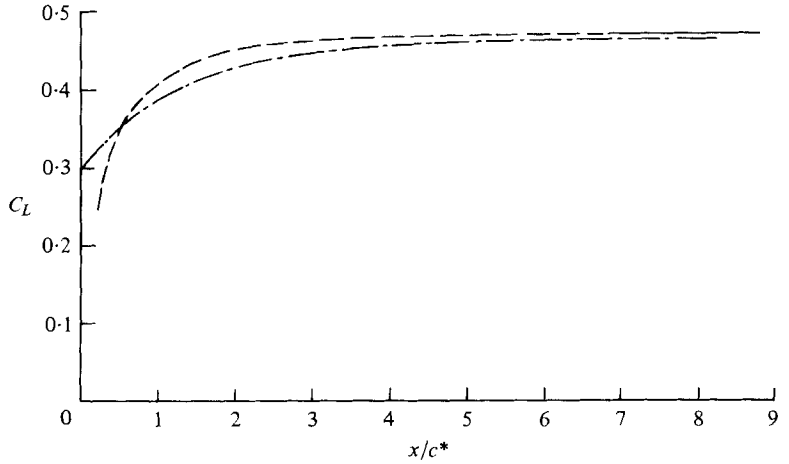

FIGURE 3. Lift coefficient variation with distance travelled from rest in fixed wing flight ($\alpha_0 = 0{\cdot}1$ rad, $A = 6$, elliptic wing). ——, lifting line ($x/c \to \infty$); – – –, present method; —·—, Jones (1940).

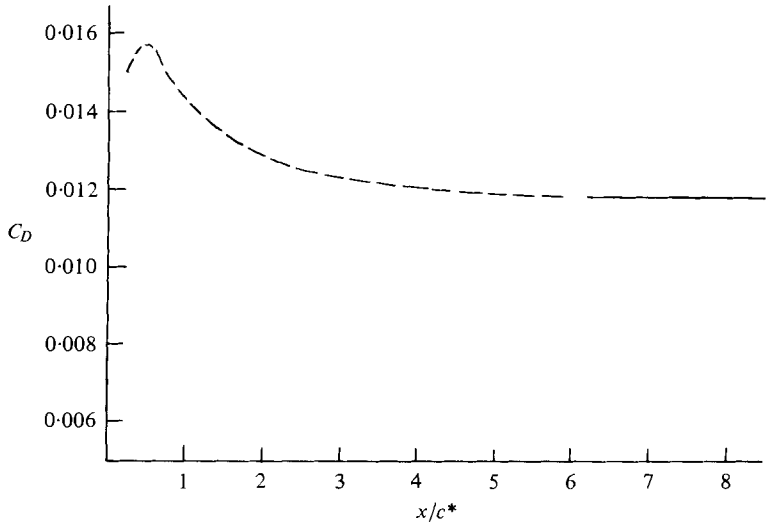

FIGURE 4. Induced drag coefficient variation with distance travelled from rest in fixed wing flight ($\alpha_0 = 0{\cdot}1$ rad, $A = 6$, elliptic wing). ——, lifting line ($x/c \to \infty$); – – –, present method.

The present method also gives the induced drag coefficient, shown in figure 4, which was not calculated by Jones. The induced drag has the correct limiting values at $x/c^* = 0$ and $x/c^* \to \infty$. Just after the start of the motion we find that the induced drag is larger than its final value because of the proximity of the starting vortex.

The final test case is a pair of untwisted wings in flapping flight with both the wing incidence α_0 and the incidence θ of the body axis equal to zero. The lift developed during the upstroke is then expected to be the opposite of that developed during the downstroke. The thrust against time curve, on the other hand, is expected to be the same for each of the two strokes. The variation of the forces is expected to be smooth.

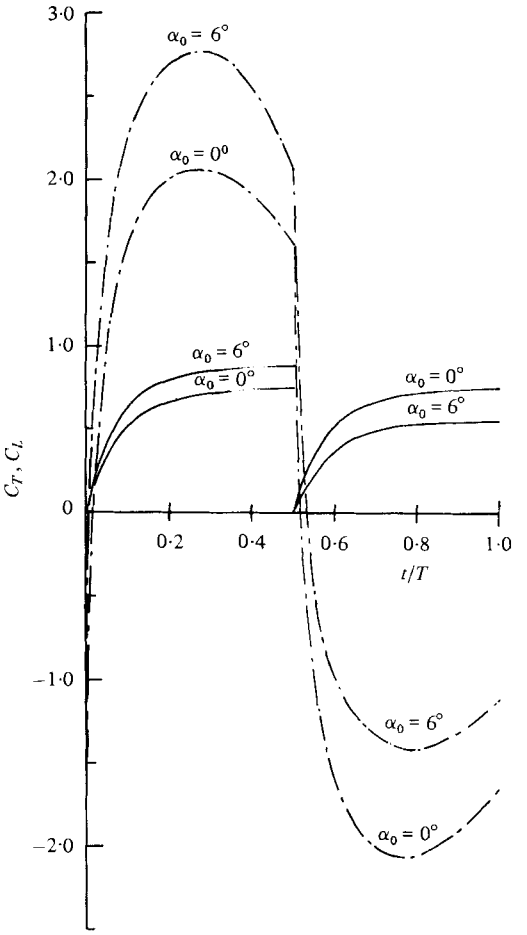

FIGURE 5. Variation of the thrust and lift coefficients C_T and C_L throughout one complete period of the flapping motion ($\nu = 2$, $\beta = 80°$, $\theta = \gamma = 0°$). ——, C_L, — — —, C_T.

The numerical results, shown in figure 5, have the desired characteristics. In addition, they demonstrate that when α_0 is not zero ($\alpha_0 = 6°$ in the example shown) a net lift is developed and different amounts of thrust are produced on the upstroke and downstroke.

5.2. *Unsteady and three-dimensional effects*

The neglect in previous work of the unsteady and the three-dimensional effects was a major reason for undertaking the present study. In this section we propose to identify these effects by examining some numerical examples of the instantaneous forces. The parameters determining the magnitude of the unsteadiness and the three-dimensionality are the frequency parameter and the flapping amplitude respectively. The relationship between both the average forces and the efficiency and these parameters will be the subject of the next section.

The effect of the unsteady aerodynamics is best demonstrated by considering the thrust coefficient as a function of time. Since the approximate quasi-steady analyses

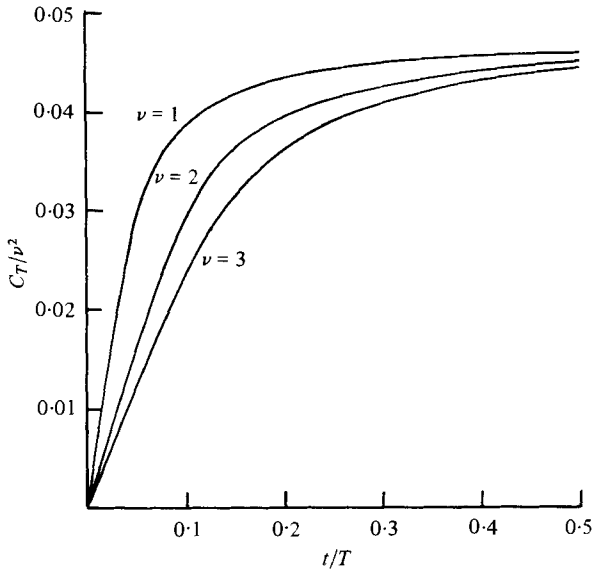

FIGURE 6. Variation of C_T/ν^2 with dimensionless time t/T during one stroke at different frequency parameters for the Oehme & Kitzler (1975) planform ($A = 10, \beta = 40°, \alpha_0 = \gamma = \theta = 0°$).

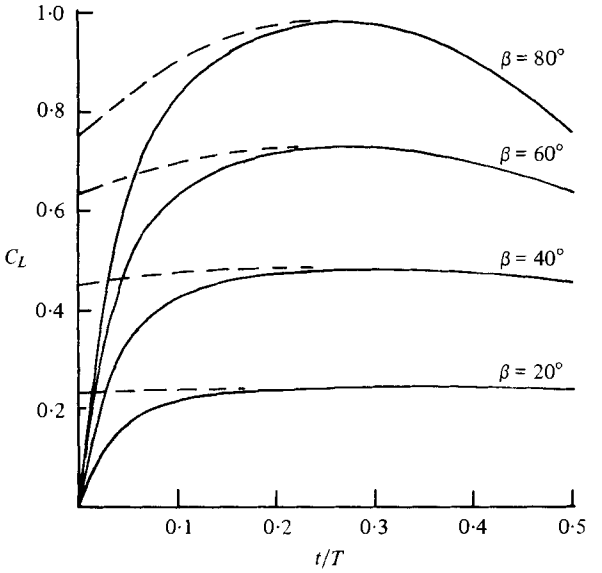

FIGURE 7. Variation of the lift coefficient C_L with dimensionless time t/T during one stroke for different flapping amplitudes β for the Oehme & Kitzler (1975) planform ($A = 10$, $\nu = 1$, $\alpha_0 = \gamma = \theta = 0°$). ——, present method (unsteady); – – –, quasi-steady ($\nu \to 0$).

presented in the appendix suggest that $C_T \propto \nu^2$, we plot C_T/ν^2 in figure 6 as a function of t/T (T = flapping period) for the case where there is symmetry between the downstroke and the upstroke, i.e. $\alpha_0 = \gamma = \theta = 0°$. The curves support the parametric predictions in that, for sufficiently large times, $C_T/\nu^2 \to$ constant. The unsteady effects manifest themselves in the finite rate of increase of C_T at the beginning of the

stroke, due largely to the proximity of the transverse vortex. As the frequency increases, the build-up of the thrust takes an increasing part of the stroke. A consequence is that, if $\bar{C}_T \propto \nu^x$, then $x < 2$, and this will later be seen to affect the efficiency.

The most obvious three-dimensional effect is that on the lift coefficient. It is shown in figure 5 that, whereas the thrust (and power) coefficients tended toward constant values at the end of each stroke, the lift coefficient reached a maximum and then decreased significantly. The explanation of this phenomenon is that the lift is the vertical component of the normal force, $C_L \simeq C_N \cos\phi$. When the effect of the transverse vortex has subsided, $C_N \simeq$ const., and hence so are C_T and C_P, and $C_L \propto \cos\phi$. This is demonstrated in figure 7, showing the lift coefficient (full line) as a function of time for different flapping amplitudes, all other variables being kept constant. Each of the dashed curves represents a constant times $\cos\phi$ and shows the variation of C_L during a cycle which would be obtained from a quasi-steady analysis.

The emphasis throughout the present work has been on a flapping model which incorporates constant angular velocity up- and downstrokes. Many experimental situations correspond more closely to sinusoidal motion and sample calculations were carried out using a modified computer code to represent this situation. The method for the constant angular velocity motion was designed to deal with a situation in which the bound circulation increased monotonically. It was found to be unsuitable for the sinusoidal motion in which the circulation increased and then decreased during a single stroke. For this case, the bound circulation was assumed to remain constant during the second half of the stroke and was shed at the end of the stroke. Numerical results showed that both $C_T(t)$ and $C_P(t)$ varied approximately as $\sin^2\omega t$ and that the average values $\bar{C}_T$ and $\bar{C}_P$ were little different from those for the constant angular velocity motion. Although still present, the unsteady effects on the variation of the aerodynamic forces with time (shown for the constant angular motion in figure 5) are less evident due to the inherently sinusoidal variation of $C_T(t)$ and $C_P(t)$.

5.3. *Parametric results*

Using numerical examples of the theory described in §4, we now examine the dependence of the average forces, the average power, and the efficiency on the kinematic and geometric parameters. The kinematic parameters considered are the frequency parameter ν, the flapping amplitude β, and the set incidence α_0. The geometric parameters are the wing shape and the aspect ratio, A. Parametric results have been obtained by Küchemann & Weber (1953), using a quasi-steady theory for the cases of a heaving wing and a high-advance-ratio propeller, both of elliptic planform. Under the quasi-steady assumption, the wings were elliptically loaded, and Küchemann & Weber found that

$$\bar{C}_L = \frac{2\pi\alpha_0}{1+2/A} = C_{L0}, \tag{13}$$

$$\bar{C}_T = \frac{\pi}{(1+2/A)^2}\frac{a^2\omega^2}{U^2} - \frac{\bar{C}_L^2}{\pi A}, \tag{14}$$

$$\eta = A/(A+2)$$

for the sinusoidally oscillating wing, where C_{L0} is the steady-state lift coefficient, a is the amplitude of the heaving motion and η is the efficiency. Note that our definition of the thrust coefficient differs from that of Küchemann & Weber, in that it

includes all the horizontal forces except those arising because of viscosity. Further parametric results are derived in the appendix using an approximate quasi-steady theory.

The planform used in all the calculations, except those exploring the effect on efficiency of different planforms, is that described by Oehme & Kitzler (1975). It has a constant chord along the inner half of each wing and a parabolically decreasing chord along the outer half,

$$c = c_0 \quad \text{for} \quad 0 \leqslant r \leqslant 0{\cdot}5,$$
$$c = 4c_0 r(1-r) \quad \text{for} \quad 0{\cdot}5 \leqslant r \leqslant 1.$$

According to Oehme & Kitzler, this planform shape gives a good representation of that of many types of bird.

Consider first the average lift coefficient $\bar{C}_L$. Lift can be obtained either by setting the wing hinge axis (body axis) at an angle θ relative to the flight path, or by setting the wing at an angle α_0 to the wing hinge, or by any combination of these two modes. Results of calculations for $\bar{C}_L$ for a frequency parameter $\nu = 1$ and flapping amplitude $\beta = 40°$ have been compared with the steady-state lift coefficient over a range of angles of incidence. The principal features of the results were the linear relationships between $\bar{C}_L$ and incidence for the flapping wing, the small difference ($< 2\,\%$) in the values of $\bar{C}_L$ at a given incidence for the steady and flapping wings, and the small differences ($< 1\,\%$) resulting from the use of either α_0 or θ. The consequences of using α_0 or θ are discussed in the appendix and here we concentrate on the effects of frequency and amplitude. Küchemann & Weber predict that the average lift is independent of ν and β, i.e. $\bar{C}_L = C_{L0}$, which is equivalent to the small flapping amplitude limit of the quasi-steady result

$$\bar{C}_L = \frac{\sin \frac{1}{2}\beta}{\frac{1}{2}\beta} C_{L0} \tag{15}$$

derived in the appendix.

Figure 8 shows the effect of ν and β on $\bar{C}_L$ according to our unsteady theory and the above quasi-steady results. We see that $\bar{C}_L = C_{L0}$ gives correctly the small-amplitude limit, whereas (15) gives the low-frequency limit, which is also the lower bound for the lift. It is clear, however, that the mean lift may be significantly different from the quasi-steady value. In particular, we see that $(\partial \bar{C}_L/\partial \nu)_\beta$ is always positive; $(\partial \bar{C}_L/\partial \beta)_\nu$ on the other hand is negative for small ν and increases with ν. This, then, is a significant difference between our unsteady theory and the quasi-steady approximations. Since the difference between the quasi-steady and the unsteady theories lies in the treatment of the vortex wake, we are led to conclude that in the unsteady theory the induced velocity field is such as to result in a higher average lift coefficient.

Next we consider the relationship between the average thrust coefficient C_T and the frequency parameter ν, the flapping amplitude β, and the incidence α_0. Using the results (13) and (14) for heaving wings and replacing the heaving amplitude a by the flapping amplitude β, the quasi-steady theory predicts that $\bar{C}_T = a\nu^2\beta^2 - b\alpha_0^2$, where a and b are constants. In §5.2, we argued that $\bar{C}_T \propto \nu^x$ with $x < 2$ because of the unsteady aerodynamics. Figure 9 shows log–log curves of $\bar{C}_T$ as a function of ν at different flapping amplitudes. The slope of the curves correspond to the exponent x, and increases from $x = 1{\cdot}81$ when $\beta = 20°$ to $x = 1{\cdot}95$ when $\beta = 120°$. The rise of

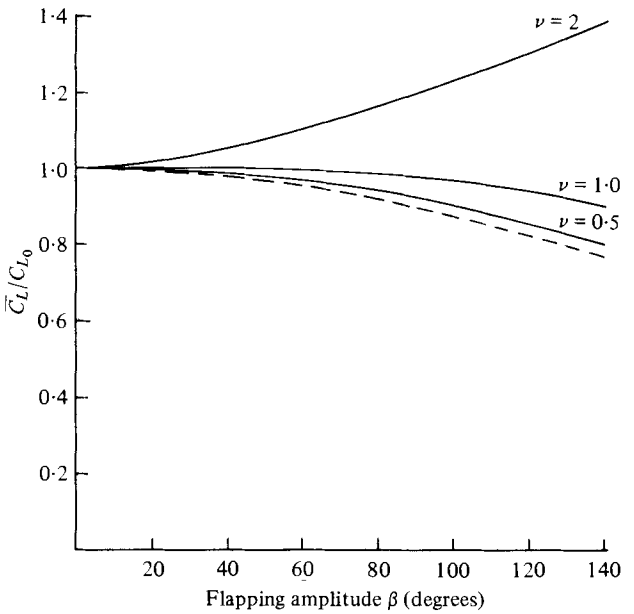

FIGURE 8. The effect of flapping amplitude β and frequency parameter ν on the average lift coefficient. ——, present method (unsteady); – – –, quasi-steady ($\nu \to 0$).

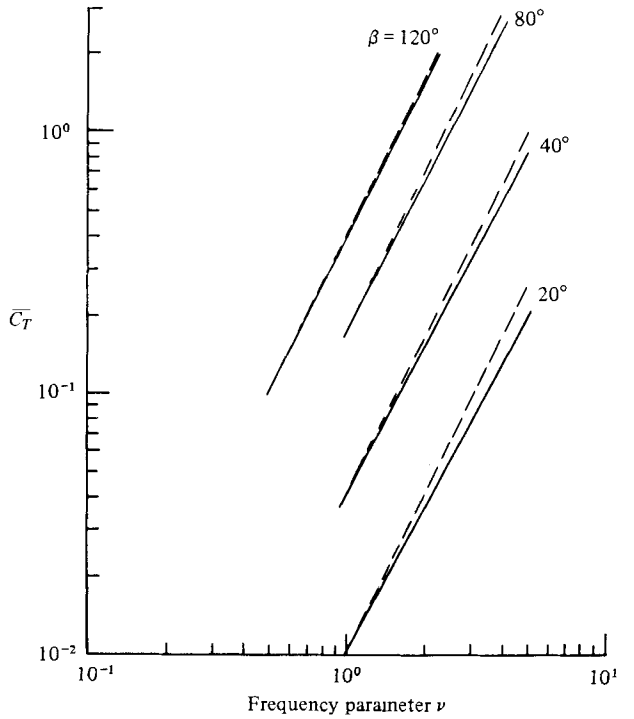

FIGURE 9. Variation of the average thrust coefficient $\bar{C}_T$ with frequency parameter ν for various amplitudes. ——, present method; – – –, $\bar{C}_T \propto \nu^2$.

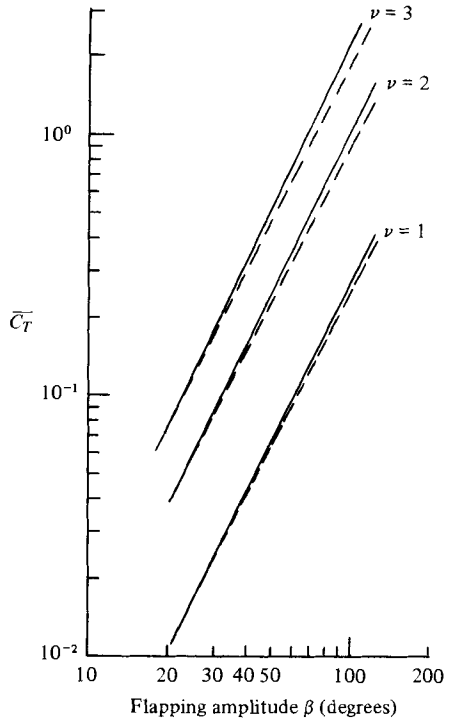

FIGURE 10. Variation of the average thrust coefficient $\bar{C}_T$ with flapping amplitude β for various frequency parameters ν. ——, present method; – – –, $\bar{C}_T \propto \beta^2$.

the exponent with flapping amplitude is explained by the increase of the average distance of the wing from the starting transverse vortex with β, which results in smaller induced velocities and hence a larger thrust. The average thrust coefficient $\bar{C}_T$ is shown as a function of β for different values of ν in figure 10. In this case the exponent ζ in $\bar{C}_T \propto \beta^\zeta$ is seen to increase from $\zeta = 2{\cdot}01$ when $\nu = 1$ to $\zeta = 2{\cdot}15$ when $\nu = 3$. According to the quasi-steady theory the exponent ζ should be equal to 2. The variation of $\bar{C}_T - (\bar{C}_T)_{\alpha_0 = 0}$ with the incidence α_0 was found to be

$$C_T - (C_T)_{\alpha_0 = 0} \propto \alpha_0^{2{\cdot}1},$$

whereas the quasi-steady theory predicts it is proportional to α_0^2.

In each of these cases of the variation of $\bar{C}_T$ with ν, β and α_0, the numerical calculations result in values of the exponent of $2 + \epsilon(\nu, \beta)$ where ϵ is small. The small difference between these results and the quasi-steady results, which may seem to be of little significance, will later be shown to have an important effect on the efficiency.

The relationship between the average power coefficient $\bar{C}_P$ and ν and β may be examined in a manner similar to that of $\bar{C}_T$. Figure 11 shows the variation of $\bar{C}_P$ with ν for different values of β and figure 12 the variation with β for different values of ν. The curves are now not straight lines, so that we cannot give a single value to their slope. It is clear from the graphs, however, that the slope is equal to 2 for small values of both ν and β, and deviates therefrom when either ν or β becomes large. The quasi-steady result derived in the appendix is $\bar{C}_P \propto \nu^2\beta^2$. Thus, as for previous results of the present theory, where the quasi-steady theory predicts exponents equal to 2, the results of the unsteady theory give values of $2 + \epsilon(\nu, \beta)$.

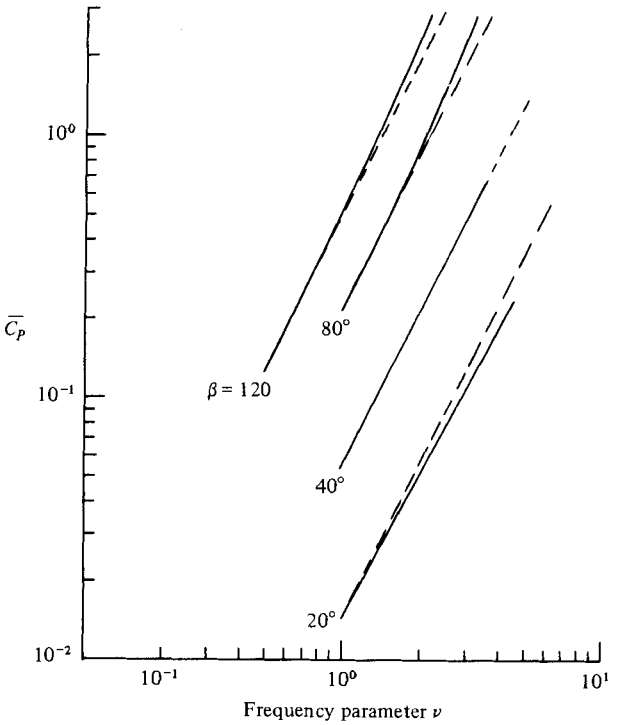

FIGURE 11. Variation of the average power coefficient $\overline{C}_P$ with frequency parameter ν for various flapping amplitudes β. ——, present method; – – –, $\overline{C}_P \propto \nu^2$.

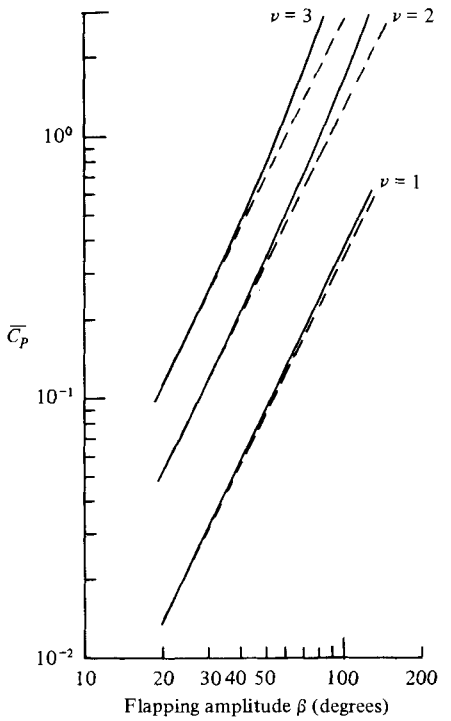

FIGURE 12. Variation of the average power coefficient $\overline{C}_P$ with flapping amplitude β for various frequency parameters ν. ——, present method; – – –, $\overline{C}_P \propto \beta^2$.

Finally, we consider the efficiency, which is defined as the ratio of the average rate of doing work by the thrust to the average power input at the wing hinges

$$\eta \equiv \overline{TU}/\overline{P} = \bar{C}_T/\bar{C}_P.$$

We restrict ourselves to the case where $\alpha_0 = \gamma = \theta = 0°$, where the flapping wings act as a purely propulsive system. Given these restrictions, the efficiency is still a function of the wing planform, the aspect ratio A, the frequency parameter ν, and the flapping amplitude β. The effect of the planform shape on the efficiency is demonstrated by calculating the efficiencies of four wings of different planforms at arbitrarily chosen values of A, ν and β, listed in table 1. The four planforms are the rectangular, the straight taper, the elliptic, and the semiparabolic planform of Oehme & Kitzler (1975). At the chosen conditions of $A = 10$, $\nu = 1$, $\beta = 40°$, the rectangular wing has the lowest efficiency, $\eta = 75{\cdot}7\,\%$. It is perhaps significant that the wing shape best describing that of birds, the semiparabolic, is one of those with the highest efficiency.

The effect of the aspect ratio on the efficiency of flapping wings is demonstrated in figure 13 for both the rectangular and semiparabolic planforms. The efficiency is found to increase with the aspect ratio; for the Oehme & Kitzler wing it increases from $\eta = 57{\cdot}8\,\%$ when $A = 4$ to $\eta = 85{\cdot}4\,\%$ when $A = 20$. The increasing efficiency of flapping flight with aspect ratio is a consequence of the decrease of the induced drag of a wing in steady flight with increasing aspect ratio. The increase of efficiency with aspect ratio has clear implications for birds. Birds such as the Swift (*Apus apus*), which spend a considerable part of the day in flapping flight, probably save a substantial amount of energy through the use of high-aspect-ratio wings.

When the wing shape and the aspect ratio are fixed, the efficiency is still a function of the frequency parameter and the flapping amplitude, as shown in figure 14. As $\nu \to 0$ the efficiency becomes independent of β, and the limiting value of 0·8 lies between the quasi-steady results for a heaving wing (0·83) and a propeller (0·72) obtained by Küchemann & Weber (1953). The quasi-steady theory does not, however, show any dependence of η on ν or β. The present study shows considerable reductions of η with ν and β, both $(\partial\eta/\partial\nu)_\beta$ and $(\partial\eta/\partial\beta)_\nu$ being negative.

The only experimental results known to us to provide parametric relationships are those of Moineau (1939) and those of Archer *et al.* (1979). Moineau tested rigid heaving wings in a water channel, but at a low Reynolds number and at frequency parameters about ten times larger than those considered here. Moineau found that the average thrust increased as the square of the frequency ω and the amplitude a, whereas the power increased as the cube of ω and a, i.e.

$$\overline{T} \propto \omega^2 a^2, \quad \overline{P} \propto \omega^3 a^3.$$

These experimental results for the thrust confirm both the classical result that rigid wings – both heaving and flapping – produce thrust (e.g. Lighthill 1974) and also the predictions of the present theoretical model regarding the variation of the thrust with frequency and amplitude. The proposed explanation for the discrepancy between the theoretical results for the power and Moineau's results is that in his experiments the power required because of the profile drag was the dominant term. Lighthill (1977) has shown that at high frequencies the power required because of the profile drag is $P \propto \omega^3 a^3$, which would explain Moineau's results. Chabonat (1970) and Fejtek &

Wing shape	η (%)
rectangular	68·7
tapered (taper ratio = 0·5)	73·1
elliptic	75·7
Oehme & Kitzler (1975)	75·7

TABLE 1. Comparison of the efficiency of different planform shapes ($A = 10$, $\nu = 1$, $\beta = 40°$, $\alpha_0 = \gamma = \theta = 0°$).

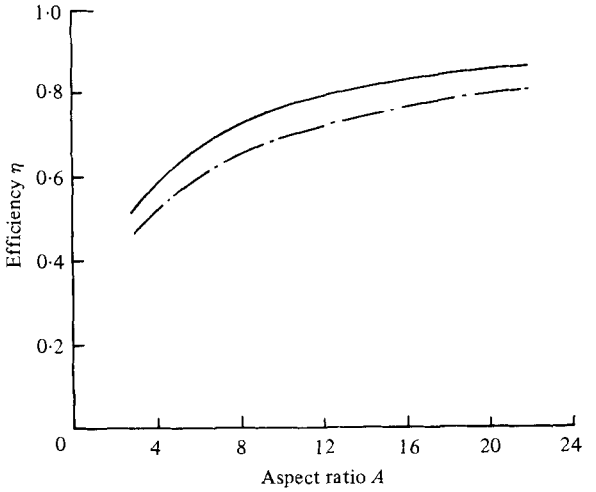

FIGURE 13. Variation of the efficiency η with aspect ratio A ($\nu = 1$, $\beta = 40°$, $\alpha_0 = \gamma = \theta = 0°$). ——, Oehme & Kitzler (1975) planform (semiparabolic); —·—, rectangular planform.

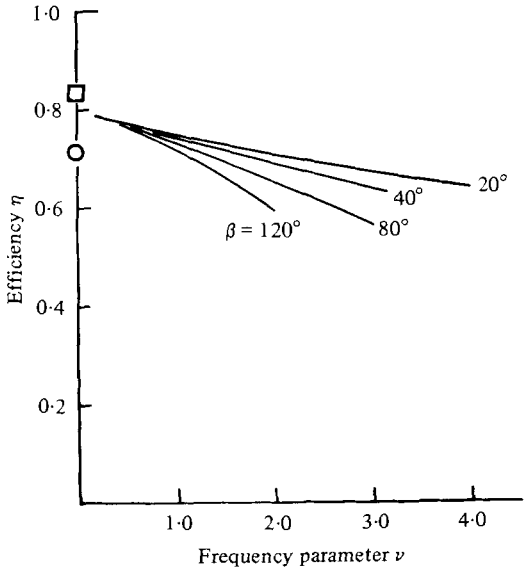

FIGURE 14. Variation of the efficiency η with frequency parameter ν for various flapping amplitudes β for the Oehme & Kitzler (1975) planform ($A = 10$, $\alpha_0 = \gamma = \theta = 0°$). □, heaving wing quasi-steady theory (Küchemann & Weber 1953); ○, propeller (Küchemann & Weber 1953).

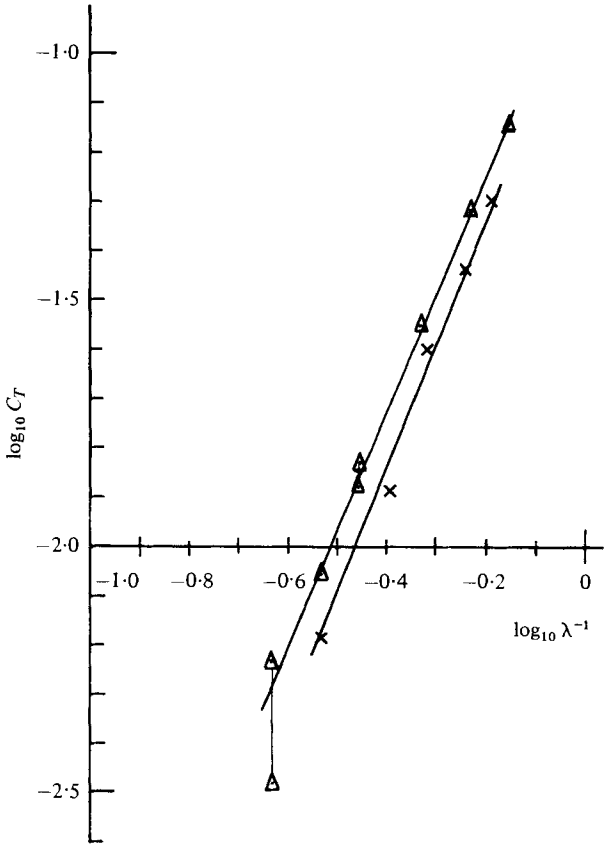

FIGURE 15. Variation of the thrust coefficient C_T with the reciprocal of the advance ratio λ from the experiments of Archer *et al.* (1979). ×, $A = 4$, $U = 10{\cdot}7$ m s^{-1}, $C_T \propto (1/\lambda)^{2{\cdot}5}$; △, $A = 6$, $U = 10{\cdot}7$ m s^{-1}, $C_T \propto (1/\lambda)^{2{\cdot}38}$.

Nehera (1980) also obtained significant drag reductions from heaving or flapping rigid wings in wind tunnels but their parametric trends are less clear.

Archer *et al.* (1979) tested a flexible flapping wing in a wind tunnel at frequencies up to 7 Hz, amplitude up to 30° and Reynolds numbers based on wing chord up to 10^5. They describe their results in terms of the advance ratio λ where $\lambda \propto 1/va$. In order to compare their results with the present study their data have been replotted to show the variation of the thrust coefficient as a function of $1/\lambda$, as shown in figure 15. We find that $C_T \propto (va)^{2{\cdot}38}$ for $A = 6$, and $C_T \propto (va)^{2{\cdot}5}$ for $A = 4$. The differences between these exponents and the predicted values of 2 may be due to the twist flexibility of the wings of Archer *et al.* and to the effect of profile drag described earlier.

6. The power curve for birds

In this final section the theory developed earlier is applied to the steady forward flight of birds. We shall calculate, as numerical examples, the power required for aerodynamic purposes as a function of forward speed for two different birds, the

Pied Flycatcher (*Ficedula hypoleuca*), and the Domestic Pigeon (*Columba livia*), for which the results of previous theoretical work have been described by Rayner (1979*b*).

It is appropriate to review the basic assumptions of the model to be used for these calculations in the context of the application to bird flight. The essential assumption is that of inviscid flow, used to establish the unsteady lifting line method. The aerodynamic forces acting on the flapping wing are calculated using this method independently of any viscous effects. In steady flow this is justified when the Reynolds number is large. For the case of bird flight, where the Reynolds numbers are in the range $10^4 < Re < 10^6$ (Nachtigall 1977), the assumption of the independence of inviscid and viscous effects would be justified in steady flows such as gliding flight. However, study of the dynamic stall of aerofoils (McCroskey 1975; Mehta 1977; Maresca, Favier & Rebont 1979) has shown that in unsteady flow complex boundary-layer effects result in a strong coupling between inviscid and viscous phenomena. In particular, the average lift can exceed its steady-state counterpart considerably as a result of the lift curve extending beyond the steady-state stalling incidence (Maresca *et al.* 1979). As a first approximation, therefore, the dynamic viscous effects may be accounted for in the unsteady lifting line method by removing the restriction that the local incidence should be less than the steady flow stalling incidence.

The second assumption made in the description of the flow is that the unsteadiness is accounted for by considering the unsteady induced velocities, but neglecting the virtual mass effect. In the case of bird flight, Von Holst & Küchemann (1942) have shown that the frequency parameter $\nu(=\omega s/U)$, based on the semispan, is of order one. The frequency parameter based on the semichord, which is relevant to virtual mass effects, will then be about one order of magnitude lower, and virtual mass effects will therefore be small. It is also assumed that the inertial power associated with deceleration of the wings at the end of each stroke is negligible. Weis-Fogh (1973) and Cloupeau *et al.* (1979) have shown that it is a significant contribution to the power consumption of insects, but following Rayner (1979*b*) we concluded that, for the increased scale of birds, it is a negligible term. Finally, we make the assumption of an incompressible fluid. This clearly applies to bird flight, where the highest recorded sustained speed in level flight is a remarkable 47 m/sec (Lighthill 1974).

One can readily observe that the wings of most birds have little or no sweep, and Greenewalt (1962) has shown that their aspect ratios lie between 5 and 18. Such wings satisfy the assumptions of the lifting line theory which is used in the present study. The assumption of constant angular velocity of flapping $\dot{\phi}$ is clearly not exact in the case of bird flight, although Brown (1953) and Wilding (1961) have shown that $\dot{\phi}$ is approximately constant during a large part of the downstroke, there being a rapid deceleration at the end of it. The kinematics of the upstroke are often more complex, but, since the loading of the wings is much lower than during the downstroke, their accurate modelling may be of less importance.

The active variation by birds of parameters such as variable wing camber, twist and span is not considered in the model. Special features of bird wings such as chordwise flexibility or wing porosity are also neglected. Previous theories have also ignored these effects, and in addition all the earlier theories were quasi-steady. Our aim, then, is to obtain estimates of the instantaneous forces on a bird and to estimate the power requirement according to an unsteady theory, given a set of data which

characterize the bird, using an estimated drag. These power estimates can then be compared with those of the more recent quasi-steady theories.

The balance of forces required for steady level flight can be achieved by different combinations of the kinematic parameters, but for our present calculations we adopted a single systematic procedure. We assume the mass, the geometry and the flapping frequency are known, the latter being taken to be constant (Rayner 1979*c*; Goldspink 1977). The wings are untwisted, uncambered and set at zero degrees relative to the wing hinges. The only remaining free parameters then are the flapping amplitude β, and the body axis angle θ. The final balance of forces is approached by successive approximations, through adjustments to the values of β and θ. This arbitrary method is not necessarily the most efficient one, but the results will nevertheless include the features resulting from the unsteady nature of the flow. The drag forces are evaluated using Rayner's (1979*b*) method (his equation (5) for the parasite drag).

The power curves for the Pied Flycatcher (*Ficedula hypoleuca*) and the pigeon (*Columba livia*) were calculated as numerical examples of the method described in §4 using the data of table 2 and the results are shown in figures 16 and 17. The figures also show Rayner's (1979*c*) results, and those calculated using Pennycuick's (1975) theory. The three curves are strictly not directly comparable, because different definitions of the power are used. In the present study and in Rayner's work, the power is defined as the rate of work expenditure to sustain the flapping motion. Rayner calculates this by considering the fluid kinetic energy in the far wake, whereas in the present study we examine the torque about the wing hinge. In Pennycuick's definition, the power is the rate at which the average aerodynamic forces do work.

We compare the curves obtained by the three methods according to three criteria: (1) the minimum power, (2) the minimum power speed, and (3) the parametric trends, $P \propto U^x$. The apparent agreement between the three values of the minimum power is somewhat misleading because of the different definition used in Pennycuick's theory. If the propulsive efficiency is taken into account then Pennycuick's minimum power is some 40–60 % above the present one. The minimum power speeds also differ widely, Rayner's being only one half of that predicted by the present method. Pennycuick's curves are shallow, so that powers close to the minimum are found over a wide range of speeds. In the present calculations we found that at high speeds $P \propto U^x$, where x is slightly smaller than 3. In Rayner's calculations the power increases approximately linearly with speed at high speed, and Pennycuick's results take on intermediate positions. We conclude, then, that there are important qualitative differences between the results obtained by the three methods.

We shall now attempt to find explanations for the differences between the curves. Three major factors differentiate the work of Pennycuick from that of Rayner and from the present study, viz. (*a*) the absence of unsteadiness in Pennycuick's model, (*b*) the different forms of treatment of the profile power (Rayner 1979*b*), and (*c*) the different definition of the power. These factors are important enough to cause large qualitative differences, but we shall not examine them in detail. It is somewhat surprising that Rayner's results should be very different from those obtained in the present study, since Rayner uses the same definition of the power and does allow for the unsteadiness of the aerodynamics to some extent by considering a discrete wake. The difference is attributed, at least in part, to the different modelling of the body

	Pigeon	Pied Flycatcher
mass m (kg)	0·4	0·012
semispan s (m)	0·335	0·115
wing area S (m^2)	63×10^{-3}	9×10^{-3}
flapping frequency f (Hz)	5·5	14·3
aspect ratio A	7·13	5·88

TABLE 2. Bird characteristics used in the numerical calculations.

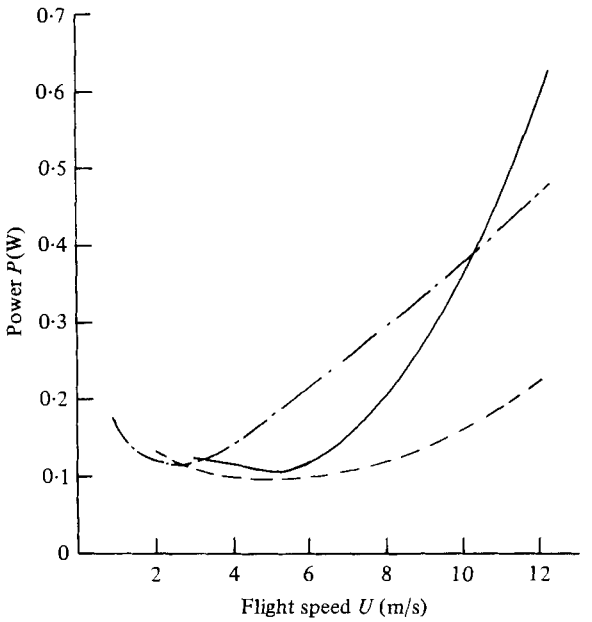

FIGURE 16. Variation of the power P with steady flight speed U for the Pied Flycatcher calculated using the data of table 2. ——, present method; —·—, Rayner (1979*c*); – – –, Pennycuick (1975).

axis inclination θ. In the present method the body axis is perpendicular to the plane in which the wings flap. The angle θ is approximately inversely proportional to U^2, and is small except at low speeds. In Rayner's method the body axis inclination θ is related to the stroke-plane angle γ through relationships of the form

$$\theta = \text{constant} - \gamma.$$

As forward speed increases, γ increases and the body inclination decreases. Rayner has experimented with a range of values of the constant given by $45° \leqslant \text{constant} \leqslant 80°$.

Although no explicit values of body axis inclination resulting from Rayner's (1979*b*, *c*) calculations are quoted, they appear in general to be fairly large, whereas in the present work they were small. The effect of this on the power is demonstrated by the quasi-steady parametric predictions for the power curve, developed in the next paragraph.

The approximate parametric dependence of the power on the forward speed can be

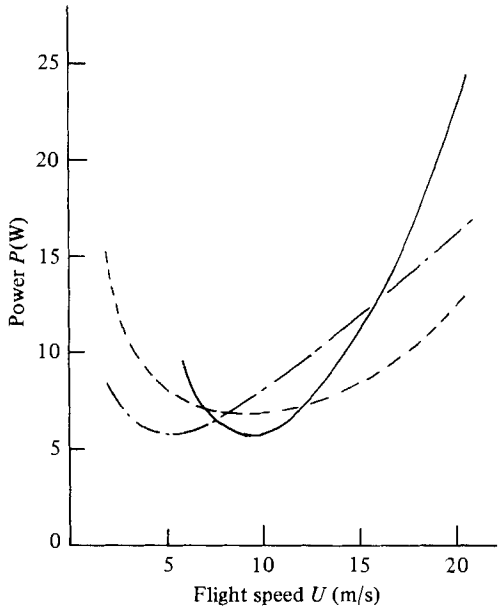

FIGURE 17. Variation of the power P with steady flight speed U for the pigeon calculated using the data of table 2. ——, present method; —·—, Rayner (1979*c*); – – –, Pennycuick (1975).

obtained from the quasi-steady parametric relationships for the forces. For the average thrust coefficient we have

$$\bar{C}_T = a\nu^2\beta^2 - b\theta^2,$$

where a and b are constants, using the equivalence of α_0 and θ for small β. The approximate form of the drag coefficient used by Rayner and in the present study is

$$C_D = c + d\theta$$

for small θ, where c and d are constants. The balance of the horizontal forces then requires that

$$a\nu^2\beta^2 - b\theta^2 = c + d\theta.$$

Since the frequency is constant, the frequency parameter is inversely proportional to forward speed, $\nu \propto U^{-1}$. The angle θ is inversely proportional to U^2 because $\bar{L} = mg \propto \theta U^2$, where g is the acceleration due to gravity. Eliminating ν and θ then gives for β

$$\beta^2 \simeq c'U^2 + d' + b'U^{-2}.$$

The power P is given by

$$P \propto \nu^2\beta^2U^3 \simeq b''U^{-1} + d''U + c''U^3.$$

According to this approximate quasi-steady analysis the power required because of the drag has a term linearly proportional to forward speed, and due to the body axis inclination, in addition to the usual cubic term.

It is thought that in the present theory and at high speeds the cubic term in the power equation dominates, whereas in Rayner's method the linear term dominates. This view is supported by the different shape of the power curve that Rayner (1979*b*) obtains when keeping the body inclination equal to zero. In that case the power is

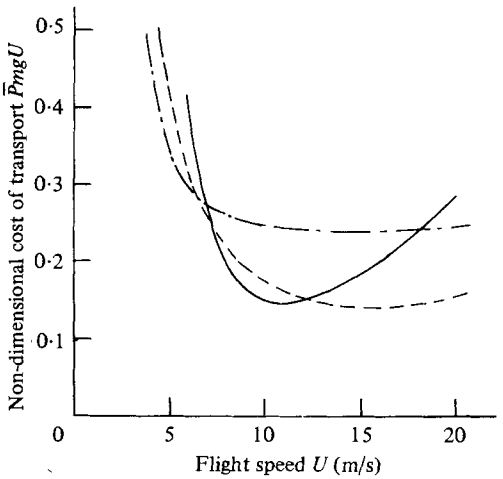

FIGURE 18. Variation of the dimensionless cost of transport with steady flight speed for the pigeon. ——, present method; —·—, Rayner (1979*c*); – – –, Pennycuick (1975).

proportional to an index somewhat larger than two at the high speed end of the curves, which is not its limiting value. We conclude tentatively, therefore, that fluid-mechanical differences between Rayner's model and the present one are masked, at present, by the effects of the different models of the body inclination.

Finally, the cost of transport C, defined as the energy expended per unit distance of travel, non-dimensionalized by dividing by the weight, $C = \bar{P}/mgU$, is shown as a function of forward speed in figure 18. The previous remarks on the power curve comparisons remain valid, and we note that the present method is the only one to exhibit a well-defined minimum for the cost of transport. The present, unsteady method predicts for the pigeon a minimum cost of transport speed of 11 m/s. Brown (1953) observed that his pigeons flew at a speed averaging 9·5 m/s which is almost identical to the predicted minimum power speed shown in figure 17 and is 14 % below the minimum cost of transport speed. Such agreement is good, considering the approximate nature of the drag estimates and the features of bird flight that have been neglected.

The results in this section demonstrate the potential of the present method to model bird flight. Fluid-mechanical differences between the present method and that of Rayner (1979*b*, *c*) are thought to be obscured by effects due to different models of the body axis inclination. There is good agreement between the calculated minimum power and minimum cost of transport speed for the pigeon and the speeds observed by Brown (1953). In the context of the present inviscid method, areas for further investigation include the body axis inclination and the extension of the present calculations to other birds.

7. Conclusion

An unsteady inviscid aerodynamic theory of rigid flapping wings in forward flight is presented. It is based on the classical lifting line method, and is therefore restricted to unswept wings of high aspect ratio. The detailed inclusion of the effects of unsteady

induced velocities, which have been omitted from previous theories of flapping wings, has shown unsteadiness to be an important aspect. The method is applicable at low values of the reduced frequency, since unsteadiness has been included to first order only.

The unsteady effects in flapping flight have been included by using a three-dimensional, unsteady model of the vortex wake; consequently the computed results are not restricted to small flapping amplitudes. Simplified limiting cases of the classical impulsively started finite-aspect-ratio wing are well modelled by the present method. Predictions relating the forces and the power to the geometric and kinematic parameters are made and compared with the limited available experimental evidence. The propulsive efficiency is estimated and found to be a function of wing geometry, frequency parameter and flapping amplitude.

Finally, the theory is applied to the flapping flight of birds, and the aerodynamic power curves for the Pied Flycatcher and for the pigeon are evaluated for comparison with previous theories. Important differences are found between the present results and those of Pennycuick (1975) and Rayner (1979*b*). Although the present results are thought to be more representative of the inherently unsteady nature of avian flight mechanics, their absolute accuracy may still be limited. Factors such as wing twist, variable geometry, viscous/inviscid interactions, wing porosity and boundary-layer control are undoubtedly important in determining the detailed aerodynamics of bird flight. However, the principal result of the present work suggests that further progress in modelling the complex phenomena associated with flapping flight will only be made by descriptions which correctly include unsteady aerodynamic phenomena.

In view of the complexity of flapping flight, particularly in regard to the application to avain flight mechanics, further progress is likely to depend on the careful evaluation of the relationships between experimental results and modelling. The extreme difficulty in carrying out precisely defined and controlled experiments on natural systems would suggest that the most profitable area for study would be wind-tunnel experiments on rigid flapping wings of simple planform and section, designed to measure time-resolved forces and power consumption. Only when the results of such experiments have been satisfactorily explained can the more complex problem of the prediction of the forces generated by the porous, flexible, variable geometry, flapping wings of birds be resolved.

The authors wish to express their gratitude for the many stimulating discussions with Professor G. M. Lilley during the course of this work and for his helpful advice during the preparation of the manuscript.

Appendix. Approximate and quasi-steady parametric analysis

We obtain a number of approximate quasi-steady dimensional relationships between the kinematic and the geometric parameters on the one hand, and the force and power coefficients on the other hand, by approximating the expressions used in the theory and considering a simple case. The principal approximation is the neglect of the induced velocities, thus making the results quasi-steady. The assumptions are that

$\gamma = \theta = 0$, that U is large, and that ν and β are small. With these assumptions and approximations we have

$$\mathbf{V}.\mathbf{n} \simeq r\nu\beta/\pi, \quad \mathbf{V}.\mathbf{l} \simeq -1, \quad \alpha \simeq \alpha_0 \pm r\nu\beta/\pi.$$

Collecting equations (1), (3), (4), (11), and using the above approximate results gives

$$C_L \simeq A\cos\phi\left(\alpha_0\pi\int_0^1 c\,dr \pm \nu\beta\int_0^1 cr\,dr\right),$$

where use has been made of $(\mathbf{V}\wedge\mathbf{m}).\mathbf{k} = -\cos\phi$ when $\theta = 0$. The instantaneous lift coefficient is thus proportional to $\cos\phi$, and its average value is

$$\bar{C}_L \simeq 2\pi\alpha_0\,\overline{\cos\phi}.$$

It is consistent to take $C_{L_0} = 2\pi\alpha_0$ since we are neglecting the induced velocities, so that

$$\bar{C}_L/C_{L0} \simeq \overline{\cos\phi} = \frac{\sin\frac{1}{2}\beta}{\frac{1}{2}\beta} \simeq 1-\frac{\frac{1}{2}\beta}{24}+\ldots$$

in the case of constant angular velocity. Note that, when $\alpha_0 = 0$ and $\theta \neq 0$, the incidence becomes

$$\alpha \simeq \tan\theta\cos\phi \pm r\nu\beta/\pi \simeq \theta\cos\phi \pm r\nu\beta/\pi$$

for small θ. The resulting average lift coefficient is

$$\bar{C}_L/C_{L_0} \simeq \overline{\cos^2\phi} = \frac{1}{2}\left(1+\frac{\sin\beta}{\beta}\right) \simeq 1-\frac{\frac{1}{2}\beta}{12}+\ldots.$$

The variation of the average lift with the body inclination θ will be less than the variation with the wing incidence α_0 according to the quasi-steady theory, although the difference will be small for small values of β.

Consider next the thrust coefficient, which, after substitution, is

$$C_T = \pi A\int_0^1 \alpha c V(\mathbf{V}.\mathbf{n})\,dr$$

when $\theta = 0$. In the high-speed, small β and ν limit, this expression becomes

$$C_T \simeq \pm\alpha_0\nu\beta A\int_0^1 rc\,dr + (A/\pi)\nu^2\beta^2\int_0^1 r^2c\,dr.$$

It follows that the average thrust coefficient increases proportionally to the square of the frequency parameter and flapping amplitude, $\bar{C}_T \propto \nu^2\beta^2$. Küchemann & Weber (1953) found a similar relation between the average thrust coefficient and the frequency and amplitude.

Finally, the non-dimensional power coefficient may be written

$$C_P = \pm A\nu\beta\int_0^1 \alpha rc V(\mathbf{V}.\mathbf{l})\,dr.$$

In the limiting case of high U and small ν and β this reduces to the same approximate expression as for C_T, and so the average power coefficient is also proportional to the

square of the frequency parameter and the flapping amplitude. According to the approximate quasi-steady theory the efficiency $\eta = \bar{C}_T/\bar{C}_p$ is independent of frequency and amplitude, as found by Küchemann and Weber.

REFERENCES

ARCHER, R. D., SAPUPPO, J. & BETTERIDGE, D. S. 1979 Propulsion characteristics of flapping wings. *Aeronaut. J.* **83**, 355–371.

BETTERIDGE, D. S. & ARCHER, R. D. 1974 A study of the mechanics of flapping flight. *Aeronaut. Quart.* **25**, 129.

BRAMWELL, A. R. S. 1976 *Helicopter Dynamics.* Edward Arnold.

BROWN, R. J. H. 1953 The flight of birds: II. Wing function in relation to flight speed. *J. Exp. Biol.* **30**, 90–103.

CHABONAT, M. 1970 Contribution à l'étude des écoulements instationnaires. *L'Aéronaut. et l'Astronaut.* **23**, 23–37.

CLOUPEAU, M., DEVILLERS, J. F. & DEVEZEAUX, D. 1979 Direct measurements of instantaneous lift in desert locust; comparison with Jensen's experiments on detached wings. *J. Exp. Biol.* **80**, 1–15.

CONE, C. D. 1968 The aerodynamics of flapping bird flight. *Virginia Institute of Marine Science, Special Scientific Report*, no. 52.

DUNCAN, W. J., THOM, A. S. & YOUNG, A. D. 1970 *Mechanics of Fluids.* 2nd edition. Edward Arnold.

ETKIN, B. 1972 *Dynamics of Atmospheric Flight.* John Wiley.

FEJTEK, I. & NEHERA, J. 1980 Experimental study of flapping wing lift and propulsion. *Aeronaut. J.* **84**, 28–33.

FILON, L. N. G. 1928 On a quadrature formula for trigonometric integrals. *Proc. Roy. Soc. Edin.* **49**, 38–47.

GOLDSPINK, G. 1977 Mechanics and energetics of muscle in animals of different sizes, with particular reference to muscle fibre composition of vertebrate muscle. Article in *Scale Effects in Animal Locomotion*, pp. 37–55. Academic.

GREENEWALT, C. H. 1962 *Dimensional relationships for flying animals. Smithson. Misc. Colln.* **144**, no. 2.

JONES, R. T. 1940 The unsteady lift of a wing of finite aspect ratio. *NACA Rep.* no. 681.

KOKSHAYSKY, N. V. 1979 Tracing the wake of a flying bird. *Nature* **279**, 146–148.

KÜCHEMANN, D. & WEBER, W. 1953 *Aerodynamics of Propulsion.* McGraw-Hill.

LIGHTHILL, M. J. 1974 Aerodynamic aspects of animal flight. *Bull. Inst. Math. Applics.* **10**, 369–393.

LIGHTHILL, M. J. 1977 Introduction to the scaling of aerial locomotion. Article in *Scale Effects in Animal Locomotion*, pp. 365–404. Academic.

MARESCA, C., FAVIER, D. & REBONT, J. 1979 Experiments on an aerofoil at high angle of incidence in longitudinal oscillations. *J. Fluid Mech.* **92**, 671–690.

MCCROSKEY, W. J. 1975 Recent development in dynamic stall. Article in *Proc. Univ. Arizona/ USAF OSR Symposium on Unsteady Aerodynamics*, vol. 1, edited by R. B. Kinney.

MCROBERT, D. M. 1980 Aerodynamic force measurements and flow visualisation of flapping wings. *Univ. Southampton, Dept Aeronautics and Astronautics*, B.Sc. Thesis.

MEHTA, U. B. 1977 Dynamic stall of an oscillating airfoil. *AGARD Fluid Dynamics Panel Symposium on Unsteady Aerodynamics*, Ottawa, Canada, Sept. 1977, paper no. 23.

MOINEAU, R. 1939 L'aile battante autopropulsive et hypersustentatrice. *Comptes Rendus, Série A*, **208**, 964–966.

NACHTIGALL, W. 1977 On the significance of the Reynolds number and the fluid mechanical phenomena connected to it in swimming physiology and flight biophysics. *Fortschritte der Zoologie* **24** (Heft 2/3).

OEHME, H. & KITZLER, U. 1975 Untersuchungen zur Flügbiophysik und Flügphysiologie der Vögel. II. Zur Geometrie des Vögelflügels. *Zool. Jb. Physiol.* **79**, 402–424. English translation, *NASA*, Washington, Feb. 1976.

PENNYCUICK, C. J. 1968 Power requirements for horizontal flight in the pigeon *Columba livia*. *J. Exp. Biol.* **49**, 527–555.

PENNYCUICK, C. J. 1975 Mechanics of flight. Article in *Avian Biology V* (ed. Farner and King), pp. 1–75. Academic.

RAYNER, J. M. V. 1979*a* A vortex theory of animal flight. Part 1. The vortex wake of a hovering animal. *J. Fluid Mech.* **91**, 697–730.

RAYNER, J. M. V. 1979*b* A vortex theory of animal flight. Part 2. The forward flight of birds. *J. Fluid Mech.* **91**, 731–763.

RAYNER, J. M. V. 1979*c* A new approach to animal flight mechanics. *J. Exp. Biol.* **80**, 17–54.

ROBINSON, A. & LAURMANN, J. 1956 *Wing Theory*. Cambridge Univ. Press.

TUCKER, V. A. 1973 Bird metabolism during flight, evaluation of a theory. *J. Exp. Biol.* **58**, 689–709.

VON HOLST, E. & KÜCHEMANN, D. 1942 Biological and aerodynamical problems of animal flight. *J. Roy. Aero. Soc.* **46**, 39–56.

WAGNER, H. 1925 Über die Entstehung des dynamischen Auftriebes von Tragflügeln. *Zeit. angew. Math. Mech.* **5**, 17–35.

WEIS-FOGH, T. 1973 Quick estimates of flight fitness in hovering animals including novel mechanisms for lift production. *J. Exp. Biol.* **59**, 169–230.

WILDING, J. 1961 Bird flight and the aeroplane. *J. Roy. Aero. Soc.* **65**, 796–799.

WOOD, C. J. & KIRMANI, S. F. A. 1970 Visualization of heaving aerofoil wakes including the effect of a jet flap. *J. Fluid Mech.* **41**, 627–640.